2-1-2004

Novel Polymerically-Modified Clays Permit the Preparation of Intercalated and Exfoliated Nanocomposites of Styrene and its Copolymers by Melt Blending

Shengpei Su
Marquette University

David D. Jiang
Marquette University

Charles A. Wilkie
Marquette University, charles.wilkie@marquette.edu

Accepted version. *Polymer Degradation and Stability,* Vol. 83, No. 2 (February 2004): 333-346. DOI.

Novel polymerically-modified clays permit the preparation of intercalated and exfoliated nanocomposites of styrene and its copolymers by melt blending

Shengpei, Su
Department of Chemistry, Marquette University, Milwaukee, WI
David D. Jiang
Department of Chemistry, Marquette University, Milwaukee, WI
Charles A. Wilkie
Department of Chemistry, Marquette University, Milwaukee, WI

Abstract

Two new organically-modified clays have been made and used to produce nanocomposites of polystyrene, high impact polystyrene and acrylonitrile–butadiene–styrene terploymer. At a minimum, intercalated nanocomposites of all of these polymers have been produced by melt blending in a Brabender mixer and, in

some cases, exfoliated nanocomposites have been obtained. The systems have all been characterized by X-ray diffraction, transmission electron microscopy, thermogravimetric analysis, cone calorimetry and the measurement of mechanical properties. These novel new clays open new opportunities for melt blending of polymers with clays to obtain nanocomposites with important properties.

Keywords

Nanocomposites, Styrenics, Fire retardancy

1. Introduction

Clay-polymer nanocomposites have been studied extensively for several years and it is now known that most properties are enhanced by the presence of a small amount of clay [1], [2]. In order to produce a nanocomposite, the clay must be well-dispersed throughout the polymer matrix. When this dispersion is not present, the material is described as either a microcomposite or as an immiscible nanocomposite; in either case the clay is acting as a filler. If the registry between the clay layers is maintained, the material is described as an intercalated nanocomposite. If this registry is lost, it is an exfoliated, known as delaminated, nanocomposite.

Most of the work that has been carried out to date has utilized montmorillonite clays. The clay usually has sodium cations to balance the negative charge that resides on the clay layers and this makes it difficult to incorporate an organic polymer between the clay layers. The usual treatment is to ion-exchange the sodium for an organophilic cation, such as an ammonium ion which contains at least one long alkyl chain. This treatment is usually sufficient to permit the polymer to insert between the clay layers.

Nanocomposites may be prepared either by a polymerization process or by melt or solution blending. The state of the material that results from each process is very dependent upon the polymer and the organic treatment. For instance, with polyamide-6 it is not difficult to prepare an exfoliated nanocomposite by melt blending [1], [3] while for polystyrene, one may not prepare nanocomposites by melt blending but only by a polymerization technique, if the ammonium salt contains only one long chain [4], [5]. For bulk polymerization, it is advantageous to have substituents on the ammonium salt that can participate in the polymerization process in order to obtain an exfoliated system [1].

In this paper we describe new organic treatments that may be applied to a clay which will enable the formation of nanocomposites by melt blending of polystyrene, PS, high impact polystyrene, HIPS, and acrylonitrile–butadiene–styrene terpolymer, ABS. In an accompanying paper we will describe melt blending of these materials with poly(methyl methacrylate), PMMA, polypropylene, PP, and polyethylene, PE [6].

2. Experimental

2.1. Materials

The majority of chemicals used in this study, including vinylbenzyl chloride, styrene, benzoyl peroxide (BPO), *N*,*N*-dimethylhexadecylamine, inhibitor removal reagents, PS (melt flow index 200 °C/5 kg, 7.5 g/10 min, *Mw*=230,000), HIPS (melt flow index 200 °C/5 kg, 6 g/10 min), were acquired from Aldrich Chemical Co. ABS (Magnum 275, 230 °C/3.8 kg, 2.6 g/10 min) was acquired from Dow Chemical Company. Pristine sodium montmorillonite was provided by Southern Clay Products, Inc.

2.2. Instrumentation

Thermogravimetric analysis (TGA) was performed on a Cahn TG-131 instrument under a flowing nitrogen atmosphere at a scan rate of 10 °C/min from 20 to 600C. All TGA results are the average of a minimum of three determinations; temperatures are reproducible to ±3 °C, while the error bars on the fraction of nonvolatile

material is ±3%. Cone calorimetry was performed using an Atlas Cone 2 instrument according ASTM E 1354-92 at an incident flux of 35 or 50 kW/m^2 using a cone shaped heater. Exhaust flow was set at 24 l/s and the spark was continuous until the sample ignited. Cone samples were prepared by compression molding the sample (20–50 g) into square plaques using a heated press. Typical results from Cone calorimetry are reproducible to within about ±10%. These uncertainties are based on many runs in which thousands of samples have been combusted [3], [5]. X-ray diffraction was performed on a Rigaku Geiger Flex, 2-circle powder diffractometer; scans were take from 2 theta 0.86–10, step size 0.1, and scan time per step of 10 s. Bright field transmission electron microscopy (TEM) images of the composites were obtained at 60 kV with a Zeiss 10 c electron microscope or a Jeol 100CX electron microscope equipped with an AMT digital system. The samples were ultramicrotomed with a diamond knife on Riechert-Jung Ultra-Cut E microtome at room temperature or cryogenic temperatures or on a Sorvall MT-2B microtome at room temperature to give ∼70 nm thick sections. PP and PE nanocomposites were cut using cryogenic conditions. The sections were transferred from the knife-edge to 600 hexagonal mesh Cu grids. The contrast between the layered silicates and the polymer phase was sufficient for imaging, so no heavy metal staining of sections prior to imaging is required. Some images were obtained using digital technology; the highest magnification cannot be achieved with this system since the resolution of the camera is limited. Mechanical properties were obtained using a SINTECH 10 (Systems Integration Technology, Inc) computerized system for material testing at a crosshead speed of 0.2 in/min. The samples were prepared both by injection molding, using an Atlas model CS 183MMX mini max molder, and by stamping from a sheet; the reported values are the average of five determinations.

2.3. Molecular weight determination

The molecular weight of the copolymer was determined by viscosity measurements. The Mark–Houwink constants [7] of PS or PMMA were used, since the copolymer was 95% PS or 95%PMMA.

2.4. Synthesis of copolymer of styrene and vinylbenzyl chloride (COPS)

In a 2000 ml beaker were placed 200 g of inhibitor-free styrene, 10 g of vinylbenzyl chloride and 20 g of benzoyl peroxide (BPO) as initiator. The beaker was covered with aluminum foil and the reaction mixture was stirred until it was completely dissolved at room temperature. The beaker was then immersed in a water bath at 70 °C with vigorously stirred until the reaction started and it was then maintained at 80 °C for 2 h. The recovered product was 220 g of a pale yellow solid with a melting range of 96–100 °C and a molecular weight of 5000±1000. ^{1}H NMR($CDCl_3$): δ 7.90–6.30 (br,96H), (aromatic) δ 4.60–4.20 (br,2H), (CH_2Cl), δ 2.10–0.60 (br, 42H) (backbone).

2.5. Synthesis of the copolymer of methyl methacrylate and vinylbenzyl chloride (MAPS)

This copolymer was prepared using the same procedure as noted for COPS, 200 g of inhibitor-free methyl methacrylate, 10 g of vinylbenzyl chloride and 20 g of BPO. The recovered product consisted of 173 g of a white solid with a melting point range of 150–170 °C with a molecular weight in the range of 5000–6000. ^{1}H NMR($CDCl_3$): δ7.35–6.95 (br, 4H), (aromatic) δ4.62–4.50 (br, 2H), (CH_2Cl), δ3.78–3.40 (br, 60H), OCH_3, δ2.10–1.62 (br, 36H), (backbone), δ1.10–0.65 (br, 54H) (methyl).

2.6. Synthesis of the ammonium salt of COPS or MAPS

To a solution of 220 g of COPS (MAPS) dissolved in 1000 ml of tetrahydrofuran (THF) in a 2 l round bottom flask, equipped with a dropping funnel, condenser and magnetically stirred was added 40 g of *N*,*N*-dimethylhexadecylamine and the mixture was refluxed for 4 h. At the conclusion of this time period, the solvent was evaporated and the precipitate was washed twice with 200 ml of ether. A total of 260 g of a sticky product was recovered. The product was dissolved in THF then precipitated by the addition of methanol; this process was repeated three times and a white solid was obtained. A new

sharp peak is seen in the NMR spectrum at about δ1.30 which may be assigned to the methylene group of the C_{16} long chain attached to nitrogen.

2.7. Preparation of the organically-modified clay

A 260 g portion of the ammonium salt was dissolved in 1000 ml of THF while 60 g of sodium montmorillonite was dispersed in 1500 ml of distilled water over 48 h. A 2000 ml portion of THF was added to the dispersed clay and vigorously stirred for 2 h. Then the ammonium salt was added dropwise to the dispersed clay. A voluminous white precipitate appears and the slurry was stirred at 50 °C for 24 h. The stirring was stopped and the precipitate was allowed to settle and the supernatant liquid was poured off and a fresh mixture of H_2O and THF (35:65) was added and the slurry was heated, with stirring, for an additional 24 h at 50 °C. Finally the slurry was filtered and the precipitate was recovered and dried in a vacuum oven at 60 °C for 48 h; 269 g of clay was recovered.

2.8. Preparation of polymer–clay nanocomposites

All the nanocomposites in this study were prepared by melt blending in a Brabender Plasticorder at high speed (60 rpm) at 190 °C for PS, HIPS and ABS. The composition of each nanocomposite is calculated from the amount of clay and polymer charged to the Brabender.

3. Results and discussion

In previous work from these laboratories, it has been shown that melt blending of the standard type of ammonium or phosphonium salts, i.e. those in which there is only one long chain of about 16 carbons, could only produce immiscible systems [4]. It was reasoned that the compatibility between the clay and the polymer must be increased, i.e., the ammonium salt must be more organophilic. The procedure that was chosen to accomplish this goal was to prepare an oligomeric ammonium salt which could then be ion-exchanged for the sodium ions within the gallery space of the clays and this should result in a quite organophilic clay. Beyer et al. [8] have previously prepared clays which contain polystyrene on the surfactant molecule. In this instance, they have produced various oligomers of amine-terminated styrene units and, after quaternization, ion-exchanged these onto the clay. The purpose of that study was to test a model for the morphological behavior of nanocomposites. In this study, copolymers of styrene with vinylbenzyl chloride or methyl methacryalte with vinylbenzyl chloride were used. The expectation was that the benzyl chloride would be able to easily quaternize an amine and that this ammonium salt could then be ion-exchanged for the sodium cations in the clay. The styrene-containing clay is refereed to herein as COPS clay while the methacrylate-containing material is called MAPS clay. The reactions that were used to prepare these ammonium salts are shown in Scheme 1.

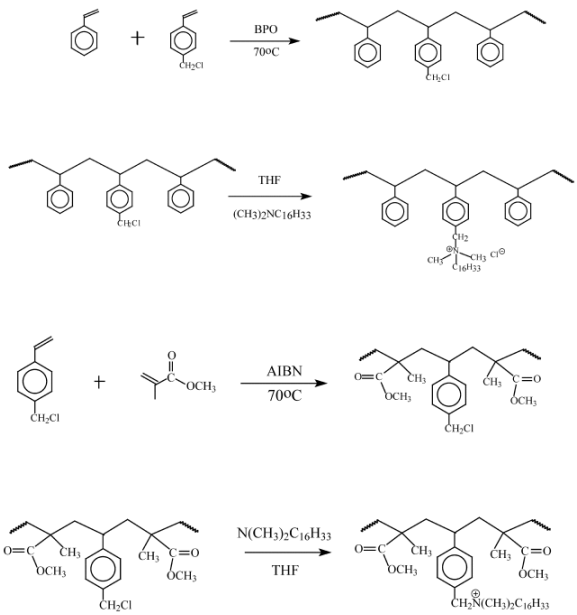

Scheme 1. Synthesis of the ammonium salts of COPS and MAPS.

The copolymer that has been prepared has a molecular weight in the range of 5000–6000 and it contains about 5 mass% vinylbenzyl chloride. This means that one mole of the copolymer contains 250–300 g of vinylbenzyl chloride and the copolymer contains 1–2 ammonium salts per unit. When the ammonium salt is reacted with the clay, it is possible that the oligomer may bridge two clay layers but it cannot bridge more than this.

3.1. XRD measurement

The *d*-spacing of the sodium clay is 1.2 nm and this increases to 8.1 nm when the ammonium salt of COPS replaces the sodium cation. The XRD results for the PS nanocomposites are shown in Fig. 1. A peak is seen near 2ϑ=1.1° for the COPS-modified clay while the peak is near 2ϑ=1.4° for all of the PS nanocomposites. The corresponding figure for MAPS-PS is shown in Fig. 2. It is obvious that the peaks in the MAPS system are broader than those of COPS, which may indicate that the MAPS-PS system is more disordered than COPS-PS.

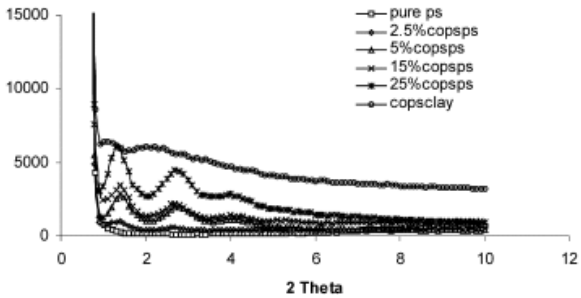

Fig. 1. XRD for COPS-PS nanocomposites.

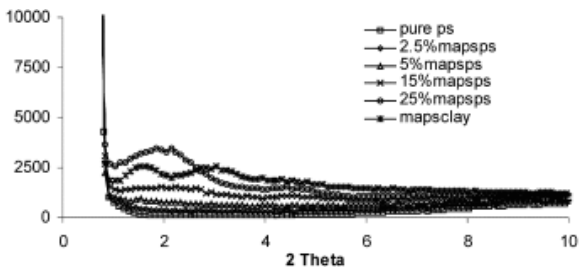

Fig. 2. XRD for MAPS-PS nanocomposites.

The reader will notice that the fraction of organically-modified clay is much larger than is normally used for nanocomposites. The molecular weight of the normal ammonium salts that are used is in the range of 400 while here the molecular weight of the ammonium salt is 5000. When an ammonium salt with a molecular weight of 400 is used, the organically-modified clay contains 22% organic and 78% aluminosilicate. Thus with 3% organically-modified clay present, there is actually 2.3% aluminosilicate present. For the ammonium slats used in this study, with a molecular weight in the range of 5000–6000, the organically-modified clay contains about 29% aluminosilicate. Thus at 25% loading of the organically-modified clay, there is 7% aluminosilicate present while at 15% loading, there is 4% alumniosilicate present.

The XRD results for the HIPS nanocomposites are shown in Fig. 3, Fig. 4; the observed 2ϑ values for COPS-HIPS are at 1.3° essentially the same as seen for the PS systems; for MAPS-HIPS, the peaks are a little higher and broader. The results for ABS are shown in Fig. 5, Fig. 6. No peaks can be seen in the XRD of COPS-ABS, suggesting either exfoliation or disordering, while a distinct and broad peak is seen with MAPS-ABS, possibly indicating intercalation.

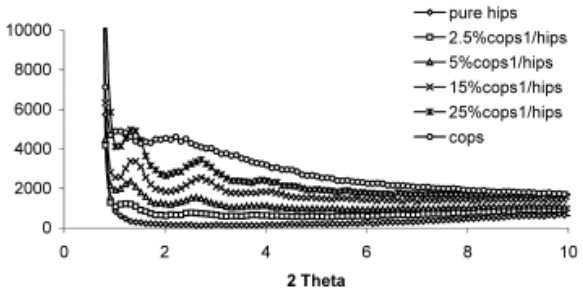

Fig. 3. XRD for COPS-HIPS nanocomposites.

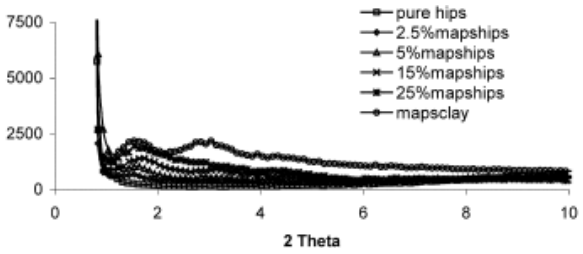

Fig. 4. XRD for MAPS-HIPS nanocomposites.

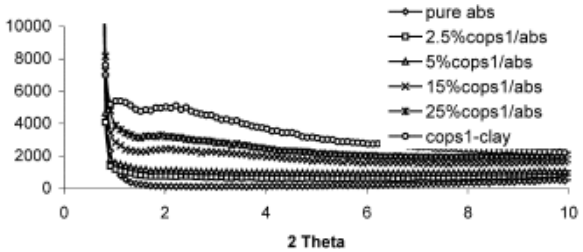

Fig. 5. XRD for COPS-ABS nanocomposites.

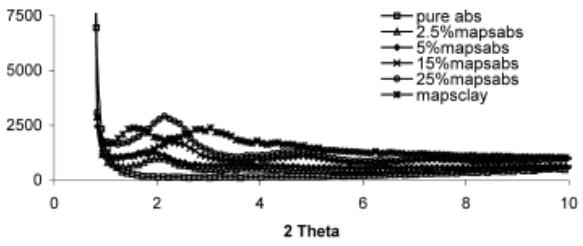

Fig. 6. XRD for MAPS-ABS nanocomposites.

The summation of the XRD results is that when peaks are seen in the XRD, they are generally broader for MAPS than for COPS; this may suggest that there is more disorder with the MAPS clay. Since all of the polymers studied herein contain aromatic rings, one may expect better compatibility with the COPS clay, which also contains the aromatic ring.

3.2. Results

The TEM images at both low and high magnification for both the organically-modified clays and the nanocomposites with PS, HIPS, ABS are shown in Fig. 7, Fig. 8, Fig. 9, Fig. 10, Fig. 11, Fig. 12, Fig. 13, Fig. 14, Fig. 15. It must be noted that some images were obtained using digital technology and this does not permit as high a magnification as is possible using film. Images that were obtained using the digital technology are shown with scale bars at 2 µm and at 100 nm while those obtained using film are shown with scale bars of 200 and 50 nm. We will consider firstly the images of the clays themselves, COPS (Fig. 7) and MAPS (Fig. 8). Nanodispersion has been achieved for COPS, but the presence of tactoids is obvious in MAPS; one can see individual layers in COPS at high magnification. The images for polystyrene may be seen in Fig. 9 (COPS) and Fig. 10 (MAPS). At the lower magnification one can see good nanodispersion for COPS but, again, the presence of tactoids is obvious in the MAPS-PS system. In the COPS system, at high magnification, one can observe single clay layers and this appears to be exfoliated or a mixture of exfoliation and intercalation. The XRD of COPS shows somewhat sharp peaks while MAPS shows broader peaks, which may be attributed to disorder and this accounts for the presence of the clay tactoids.

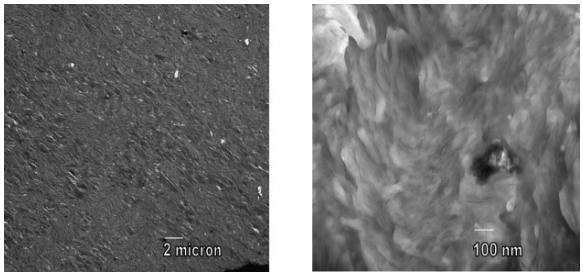

Fig. 7. TEM image at low (left) and high (right) magnification of the COPS clay.

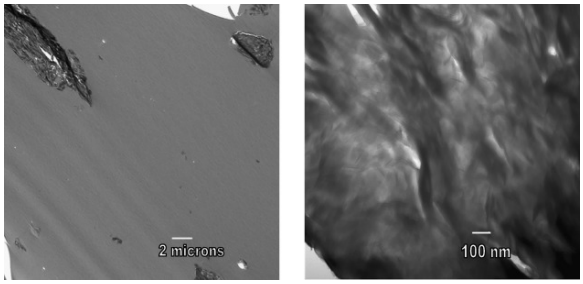

Fig. 8. TEM image at low (left) and high (right) magnification of the MAPS clay.

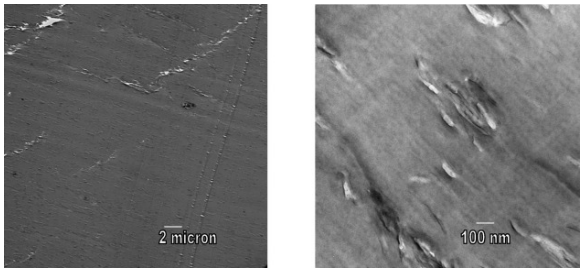

Fig. 9. TEM image at low (left) and high (right) magnification of the COPS-PS nanocomposite.

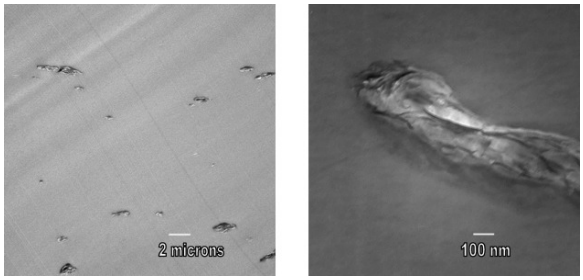

Fig. 10. TEM image at low (left) and high (right) magnification of the MAPS-PS nanocomposite.

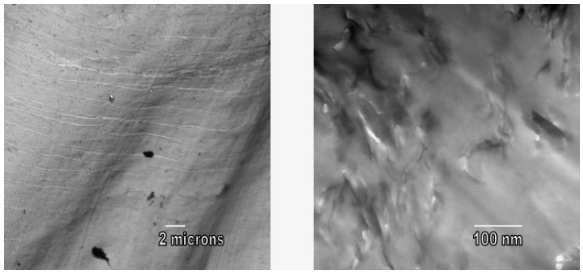

Fig. 11. TEM image at low (left) and high (right) magnification of the solution blended COPS-PS nanocomposite.

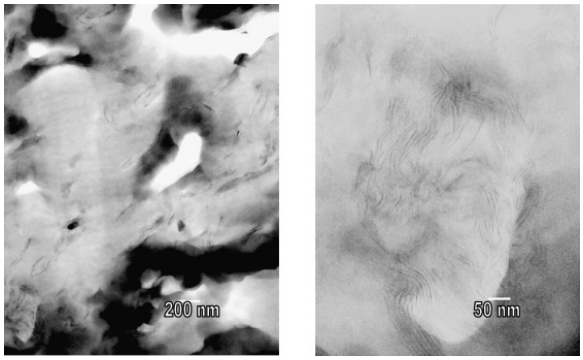

Fig. 12. TEM image at low (left) and high (right) magnification of the COPS-HIPS nanocomposite.

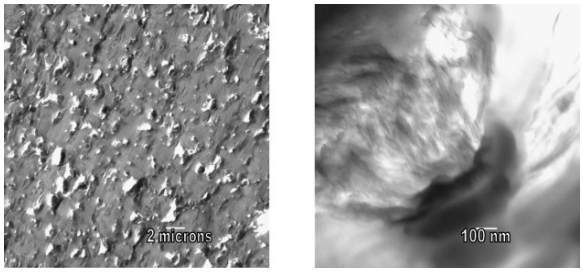

Fig. 13. TEM image at low (left) and high (right) magnification of the MAPS-HIPS nanocomposite.

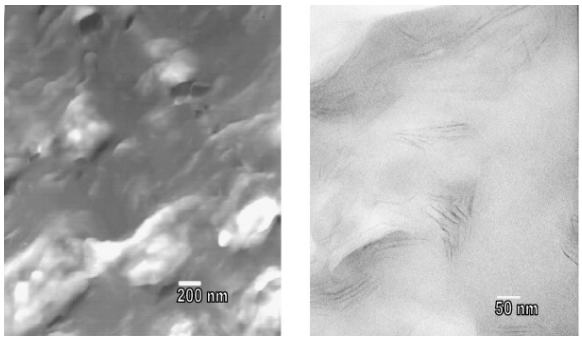

Fig. 14. TEM image at low (left) and high (right) magnification of the COPS-ABS nanocomposite.

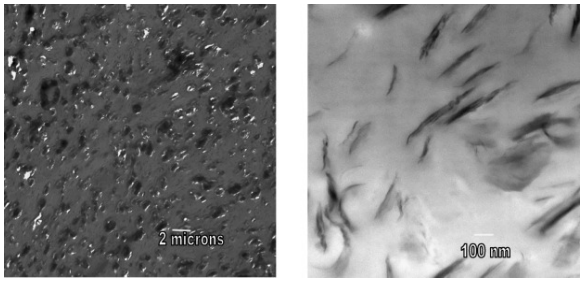

Fig. 15. TEM image at low (left) and high (right) magnification of the MAPS-ABS nanocomposite.

The COPS-PS system has also been prepared by solution blending and these images are shown in Fig. 11. Even by solution blending, there is good nanodispersion. At higher magnification, one can see the intercalated nature of this material.

The results for HIPS are quite similar for both clays, Fig. 12, Fig. 13. In both cases, there is good nanodispersion and, in the higher magnification images, one can see individual clay layers and no tactoids. The peaks in the XRD for the MAPS-HIPS system are much more pronounced than in PS and this is reflected in the TEM images. The images of ABS are similar to those of HIPS for COPS (Fig. 14) but, in the case of MAPS (Fig. 15) at higher magnification one sees mostly tactoids and not individual clay layers. The COPS-ABS system most likely should be described as exfoliated or perhaps a mixture of intercalation and exfoliation; the XRD also shows no peaks, suggesting the same conclusion.

It is clear from these results that COPS is more likely to show individual clay layers while clay tactoids are frequently observed with MAPS. The difference probably lies in the differences between styrene and methyl methacrylate. The former is a non-polar material and, as such, is unlikely to interact at all with the clay layers. On the other hand, methyl methacrylate is somewhat polar and interactions between the clay and the methacrylate may be expected. This may be sufficient to prevent the breakup of the clay tactoids and may be the reason for the difference between the two materials.

To summarize the results from XRD and TEM, intercalated nanocomposites are obtained for COPS-PS and COPS-HIPS with a mixed intercalated-exfoliated system for COPS-ABS. The MAPS clay regularly appears to give an immiscible nanocomposite for all polymers.

3.3. TGA characterization of the manocomposites

The thermal stability of the nanocomposites has been accessed using TGA; the parameters are shown in Table 1 for COPS-polymer systems and in Table 2 for MAPS-polymer systems and include the temperature at which 10% degradation occurs, a measure of the onset of degradation, the temperature at which 50%

degradation occurs, the mid-point of the degradation process, and the fraction of non-volatile material which remains at 600 °C, denoted as char[9].

Table 1. TGA data for the COPS nanocomposites

Material	T_{10} (°C)	T_{50} (°C)	Char (%)
COPS clay	367	427	27
Pure PS	370	415	2
2.5%COPS/PS	374	422	3
5%COPS/PS	394	435	3
15%COPS/PS	395	438	6
25%COPS/PS	387	438	7
Pure HIPS	414	440	1
2.5%COPS/HIPS	415	443	5
5% COPS/HIPS	416	448	6
15% COPS/HIPS	409	446	8
25% COPS/HIPS	400	445	10
Pure ABS	399	426	6
2.5%COPS/ABS	402	432	6
5% COPS/ABS	400	435	7
15% COPS/ABS	400	434	12
25% COPS/ABS	367	427	27

Table 2. TGA data for the COPS nanocomposites

Material	T_{10} (°C)	T_{50} (°C)	Char (%)
COPS clay	281	380	35
Pure PS	370	415	2
2.5%COPS/PS	347	398	2
5%COPS/PS	355	408	3
15%COPS/PS	345	400	6
25%COPS/PS	342	404	8
Pure HIPS	414	440	1
2.5%COPS/HIPS	406	440	4
5% COPS/HIPS	408	445	4
15% COPS/HIPS	382	442	17
25% COPS/HIPS	370	437	12
Pure ABS	399	426	6
2.5%COPS/ABS	397	428	7
5% COPS/ABS	392	426	7
15% COPS/ABS	390	428	9
25% COPS/ABS	385	428	13

It is very significant to note that at 350 °C, COPS clay has only undergone 7% degradation while 20% of the MAPS clay is lost by 300 °C. Thermal stability of the clays is always a concern, especially if one is to do melt blending at higher temperatures; the COPS clay may be very useful in these circumstances. TGA/FTIR studies have been

carried out on these clays and will be reported in a separate paper [10]. The initial step of the degradation is the loss of the hexadecyl group as the olefin and this suggests that quaternization of trimethylamine with the copolymer may give a clay that has even higher thermal stability.

The results for the nanocomposites are presented graphically for each of the polymer systems studied in Fig. 16, Fig. 17, Fig. 18, Fig. 19, Fig. 20, Fig. 21. It is clear from this data that the COPS clay has enhanced thermal stability relative to the MAPS clay. This is not surprising, since PS has a higher thermal stability than does PMMA. COPS-PS nanocomposites show enhanced thermal stability relative to the virgin polymer while MAPS-PS has lower thermal stability. Previous work on PS nanocomposites [11], [12], [13] has shown that nanocomposite formation invariably causes an increase in thermal stability. The thermal stability of the clay, relative to that of the polymer with which the clay has been combined, has a profound influence on thermal stability. For instance, for MAPS-HIPS, as the amount of clay increases, the temperature at which degradation occurs decrease. On the other hand, for COPS-HIPS all of the nanocomposites are more thermally stable than the virgin polymer. Thus MAPS-HIPS at 2.5 and 5% clay show TGA curves which approximately overlap with that of HIPS but at 15 and 25% clay, the temperatures are lower. This is presumably due to the increased amount of the less stable PMMA. For both COPS-ABS and MAPS-ABS, the nanocomposite is more stable than the clay and there is very little difference for each as the amount of clay is varied.

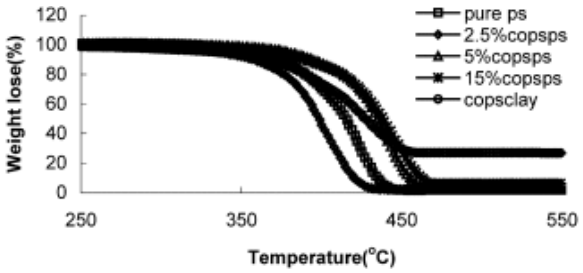

Fig. 16. TGA curves for COPS-PS nanocomposites.

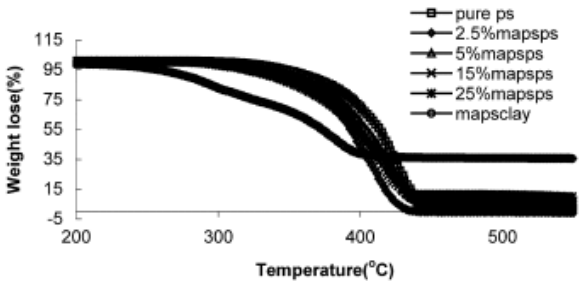

Fig. 17. TGA curves for MAPS-PS nanocomposites.

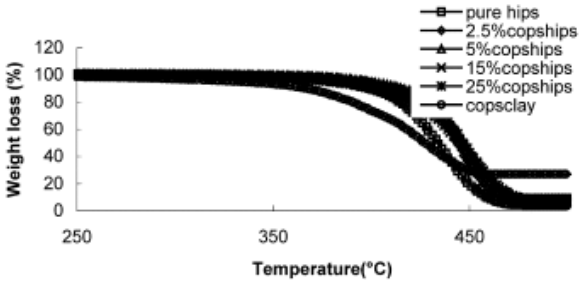

Fig. 18. TGA curves for COPS-HIPS nanocomposites.

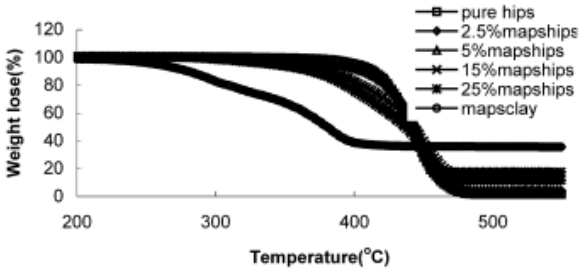

Fig. 19. TGA curves for MAPS-HIPS nanocomposites.

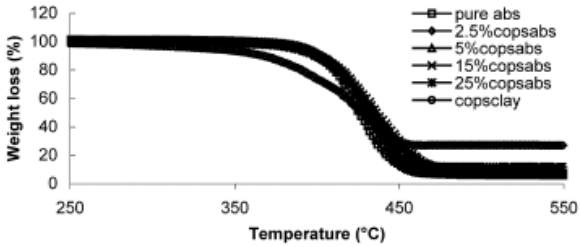

Fig. 20. TGA curves for COPS-ABS nanocomposites.

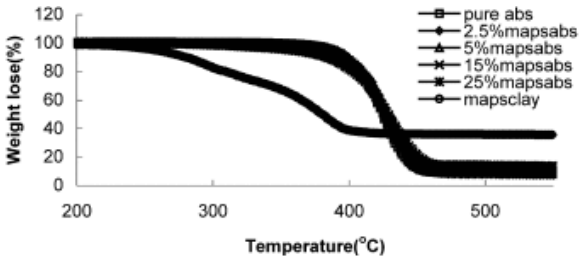

Fig. 21. TGA curves for MAPS-ABS nanocomposites.

It is significant to note that the onset temperature of the degradation is increased for COPS-PS and that all PS nanocomposites show this increase in thermal stability[11]. We are not aware of previous work on HIPS and ABS nanocomposites but there are systems, such as polyamide-6, for which the onset temperature is unaffected by nanocomposite formation [5]. Work has been carried out in these laboratories on graphite-HIPS and graphite-ABS nanocomposites and for these the onset temperatures are also unchanged [14].

A summary of the TGA results suggests that the presence of COPS clay enhances the thermal stability of all three polymers while MAPS clay does not have this effect. This may be explained by the lower thermal stability of methacrylates relative to styrenics. For some systems, most commonly styrenics, the temperature of thermal degradation is enhanced while for other polymers, such as polyamide-6, nanocomposite formation ahs no effect on TGA parameters.

3.4. Cone calorimetric characterization of the nanocomposites

The various parameters that may be evaluated using cone calorimetry, including the time to ignition, t_{ign}, the peak heat release rate, PHRR and the time to PHRR, t_{PHRR}, the mass loss rate, MLR, and the specific extinction area, SEA, a measure of the amount of smoke evolved, are tabulated in Table 3, Table 4 for polystyrene. The time to ignition for the COPS-PS system shows a relatively small decrease while the time to PHRR drops much more rapidly. Just the opposite is true for MAPS-PS, the time to ignition drops precipitously while the time to PHRR is quite constant. The amount of smoke and the total heat released are essentially the same for the virgin polymer and its nanocomposites in both systems. There is a larger reduction in PHRR and in mass loss rate for

COPS-PS than for MAPS-PS. The reduction in PHRR for COPS is as good as has been observed for any polystyrene nanocomposite [12], [13]

Table 3. Cone calorimetric data for COPS-PS nanocomposites

Composition	Pure PS	2.5%COPS/PS	5%COPS/PS	15%COPS/PS	25%COPS/PS
Time to ignition, (s)	63±5	63±6	66±1	58±2	53±3
PHRR kW/m^2 (reduction)	1253±98	1070±20 (15)	893±1 (29)	626±24 (50)	539±15 (57)
Time to PHRR, (s)	79±4	88±5	72±5	40±13	25btc6
Time to burn out, (s)	194±5	195±20	245±3	313±3	333±5
Energy released through 150 s, (MJ/m^2)	90±2	95±3	92±1	73±2	66±2
Average HRR, (kW/m^2)	465±9	486±10	379±1	275±1	248±2
Total heat released, (MJ/m^2)	90±2	95±3	93±1	86±2	83±2
Average mass loss rate, (g/s m^2)	22.7±1.6	22.5±1.8	16.8±0.5	13.3±0.2	10.3±0.3
Mass lose at 150 s, (%)	100±1	100±5	99±1	84±3	80±2
Average specific extinction area, (m^2/kg)	995±40	943±50	996±23	1109±23	1276±30

Table 4. Cone calorimetric data for MAPS-PS nanocomposites

Composition	Pure PS	2.5%MAPS/PS	5%MAPS/PS	15%MAPS/PS	25%MAPS/PS
t_{ign}, (s)	63±5	51±3	45±4	34±4	30±3
PHRR, (kW/m^2) (reduction)	1253±98	946±16 (25)	784±7 (37)	771±25 (38)	710±29 (43)
t_{PHRR}, (s)	79±4	92±5	91±5	73±11	81±14
Time to burn out, (s)	194±5	213±5	232±2	240±11	263±4
Energy released through 150s, (MJ/m^2)	90±2	86±1	83±1	83±1	79±3
Average HRR, (kW/m2)	465±9	409±2	364±2	351±3	323±15
Total heat released, (MJ/m^2)	90±2	87±1	84±1	84±1	85±4
Average mass loss rate, (g/s m^2)	22.7±1.6	21.1±0.8	16.8±0.9	17.8±0.1	16.2±2.0
Mass loss at 150 s, (%)	100±1	100±1	94±6	99±1	94±1
Average specific extinction area, (m^2/kg)	995±40	985±31	1087±10	1087±34	1037±12

The data for the HIPS nanocomposites are shown in Table 5, Table 6. Both the COPS and MAPS modified clays show a reduction in the PHRR at only 15 and 25% clay; for COPS the value is the same at each level (42% reduction) while for MAPS it is much larger at 25% (54% reduction) than at 15% (21% reduction). The total heat released is constant across the entire range of clay fractions. For COPS, the mass loss rate decreases as the fraction of clay increases and the time to ignition and the total heat released are constant across the entire range of clay fraction; a small increase in smoke is noted at the same clay amounts that produces a large decrease in PHRR. For MAPS, the time to ignition decreases rather significantly at the 15 and 25% clay levels but there is no difference in time to ignition between the two while the reduction in PHRR is much larger at 25% than at 15%. For the graphite-HIPS nanocomposite, the maximum reduction in PHRR is 37%, equivalent to what has been observed with this system.

Table 5. Cone calorimetric data for COPS-HIPS nanocomposites

Composition	Pure HIPS	2.5%COPS/HIPS	5%COPS/HIPS	15%COPS/HIPS	25%COPS/HIPS
t_{ign}, (s)	64±2	65±4	65±3	57±1	61±3
PHRR, (kW/m^2) (reduction)	1247±41	1227±17 (2)	1115±9 (11)	737±9 (41)	707±7 (43)
t_{PHRR}, (s)	54±5	51±9	38±1	26±1	25±1
Time to burn out, (s)	216±4	218±1	225±3	280±4	310±4
Energy released through 120s, (MJ/m^2)	98±3	95±1	91±1	73±1	71±1
Average HRR, (kW/m^2)	461±14	448±4	426±6	339±6	321±5
Total heat released,(MJ/m^2)	100±3	97±1	96±2	95±2	99±2
Average Mass loss rate, (g/s m^2)	20.8±1.0	18.9±0.1	17.9±0.2	14.1±0.5	12.7±0.4
Mass loss at 120s, (%)	100±1	99±1	98±1	79±2	73±1
Average specific extinction area, (m^2/kg)	1178±16	1169±19	1238±10	1358±4	1410±10

Table 6. Cone calorimetric data for MAPS-HIPS nanocomposites

Composition	Pure HIPS	2.5%MAPS/HIPS	5%MAPS/HIPS	15%MAPS/HIPS	25%MAPS/HIPS
t_{ign}, (s)	64±2	57±5	56±1	43±1	40±4
PHRR, (kW/m^2) (reduction)	1328±12	1328±17 (0)	1260±17 (9)	1050±32 (21)	607±1 (54)
t_{PHRR}, (s)	66±5	79±7	81±4	71±10	38±3
Time to burn out, (s)	206±2	208±5	208±3	233±3	300±10
Energy released through 120s, (MJ/m^2)	103±1	108±1	105±2	90±2	58±7
Average HRR, (kW/m^2)	514±2	542±6	524±8	432±9	292±7
Total heat released, (MJ/m^2)	106±1	113±2	109±2	101±2	88±1
Average Mass loss rate, (g/s m^2)	21.2±0.3	21.1±0.5	20.4±0.4	17±1	11.1±0.4
Mass loss at 120s, (%)	99±1	96±3	95±1	87±3	62±1
Average specific extinction area, (m^2/kg)	1458±18	1524±20	1507±11	1515±2	1602±33

The data for ABS are shown in Table 7, Table 8. The reduction in the PHRR is 37% for MAPS and 25% for COPS. For both systems, a reduction in PHRR is paralleled by a decrease in the mass loss rate and, for MAPS, the time to ignition decreases also at 15 and 25% clay. The amount of smoke does not change over the range of clay concentrations. For graphite-ABS nanocomposites the maximum reduction in PHRR is 48%, significantly larger than what is observed herein. This may mean that better nanodispersion of ABS is possible in graphite than in COPS or MAPS clay.

Table 7. Cone calorimetric data for COPS-ABS nanocomposites

Composition	Pure ABS	2.5%COPS/ABS	5%COPS/ABS	15%COPS/ABS	25%COPS/ABS
t_{ign}, (s)	62±6	63±1	62±1	60±5	64±1
PHRR, (kW/m^2) (reduction)	1096±56	1150±19 (0)	1017±2 (7)	865±3 (21)	816±46 (25)
t_{PHRR}, (s)	78±2	70±2	75±2	64±1	53±1
Time to burn out, (s)	219±6	216±1	221±1	230±8	233±14
Energy released through 120s, (MJ/m^2)	91±2	91±2	88±1	79±1	76±1
Average HRR, (kW/m^2)	439±5	436±10	417±1	393±1	382±3
Total heat released, (MJ/m^2)	97±1	94±2	92±1	90±1	89±1
Average Mass loss rate, (g/s m^2)	20.6±0.6	22.4±1.0	20.2±0.1	17.1±0.2	14.6±0.3
Mass loss at 120s, (%)	95±3	97±1	96±1	84±1	83±2
Average specific extinction area, (m^2/kg)	1094±19	1094±7	1120±4	1213±9	1213±8

Table 8. Cone calorimetric data for MAPS-ABS nanocomposites

Composition	Pure ABS	2.5%MAPS/ABS	5%MAPS/ABS	15%MAPS/ABS	25%MAPS/ABS
t_{ign}, (s)	62±6	65±5	64±1	55±7	51±1
PHRR, (kW/m^2)(reduction)	1096±56	1022±11 (7)	1001±56 (9)	762±19 (30)	690±35 (37)
t_{PHRR}, (s)	78±2	54±5	42±2	56±3	53±5
Time to burn out, (s)	219±6	216±2	219±3	254±2	268±2
Energy released through 120s, (MJ/m^2)	91±2	81±1	80±1	70±6	65±2
Average HRR, (kW/m^2)	439±5	388±2	381±4	326±7	303±5
Total heat released, (MJ/m^2)	97±1	83±1	83±1	83±2	81±1
Average Mass loss rate, (g/s m^2)	20.6±0.6	20.3±0.9	20.4±0.4	15.9±0.7	14.2±0.4
Mass loss at 120s, (%)	95±3	97±1	96±1	81±5	79±4
Average specific extinction area, m^2/kg	983±9	973±20	987±21	1108±42	1095±32

An observation that has previously been made by Gilman [5] and in this laboratory [15] is that a significant reduction in PHRR occurs when a nanocomposites is formed and an insignificant reduction occurs for immiscible systems. The observation of a large decrease in PHRR for the MAPS nanocomposites suggests that there is some intercalated character to these systems. A problem with TEM evaluation of the type of nanocomposite is that one samples only a very small portion of the material and infers the situation of the whole from this small sample. Since cone calorimetry samples the bulk material, it may be a more reliable indicator of nanocomposite formation than is TEM. These results provide further information to confirm this observation and suggest that one can assess nanocomposites formation by the use of the cone calorimeter and this, in combination with XRD data, is sufficient to identify intercalated, exfoliated and immiscible nanocomposites. Cone calorimetry may prove to be a technique that provides information not only on fire parameters but also enables one to ascertain the type of nanocomposite that has been produced, when used in combination with XRD data.

3.5. Evaluation of mechanical properties

The mechanical properties, including Young's modulus, tensile strength and elongation at break of all of the nanocomposites prepared in this study, together with the corresponding values of the virgin polymers have been evaluated and the data are presented in Table 9. For the most part, the presence of the clay does not have a large effect on the mechanical properties of the polymer. The kind of oligomerically-modified clay is important; MAPS behaves better than COPS in maintaining or enhancing the tensile properties of these virgin polymers. Young's modulus was increased as the amount of the clay increases for all polymers except for COPS-PS. For tensile strength, MAPS nanocomposites show better data than COPS nanocomposites. All nanocomposites show a decrease in % elongation, except MAPS-PS nanocomposites. The tensile strength decreases for COPS-PS and there is a smaller decrease for MAPS-PS; the % elongation is constant across the entire range of clay. For HIPS the tensile modulus is constant but there is a decrease in % elongation. For ABS the tensile modulus is somewhat constant to a small decrease while the elongation shows a somewhat dramatic decrease at high clay. There is some difference between COPS and MAPS but it is not a large difference.

Table 9. Mechanical properties of COPS- and MAPS-polymer nanocomposites

Nanocomposite	**Elongation(%)**	**Modulus(GPa)**	**Tensile strength (Mpa)**
Mechanical properties of polystyrene nanocomposites			
PS	2.9±0.6	1.751±0.832	31.86±10.07
2.5%Cops/PS	1.7±0.5	1.616±0.281	21.29±3.75
5%Cops/PS	2.3±0.8	1.572±0.687	17.81±3.23
15%Cops/PS	2.2±0.1	1.468±0.042	7.14±1.02
25%Cops/PS	2.1±0.2	1.751±0	7.90±0.89
2.5%Maps/PS	3.1±0.7	2.110±0.126	20.29±6.67
5%Maps/PS	3.1±0.9	1.982±0.012	33.63±4.12
15%Maps/PS	3.2±0.4	2.153±0.239	35.22±5.79
25%Maps/PS	2.6±0.7	2.455±0.043	28.65±1.66
Mechanical properties of HIPS nanocomposites			
HIPS	6.5±3.1	1.292±0.083	19.33±2.33
2.5%Cops/HIPS	5.1±2.8	1.324±0.063	20.90±1.05
5%Cops/HIPS	2.8±0.7	1.404±0.065	21.48±2.59
15%Cops/HIPS	2.5±0.4	1.693±0.223	20.41±1.89
25%Cops/HIPS	2.5±0.5	2.407±0.895	19.47±2.61
2.5%Maps/HIPS	7.2±5.0	1.298±0.040	19.67±0.80
5%Maps/HIPS	4.6±0.6	1.412±0.042	21.23±1.18
15%Maps/HIPS	4.4±1.5	1.578±0.100	19.87±1.73
25%Maps/HIPS	3.6±0.8	1.610±0.340	23.13±1.15
Mechanical properties of ABS nanocomposites			
ABS	16.8±5.3	1.426±0.019	36.49±2.27
2.5%Cops/ABS	34.8±5.8	1.355±0.028	34.18±1.38
5%Cops/ABS	25.4±4.8	1.430±0.046	34.37±0.97
15%Cops/ABS	3.5±0.5	0.927±0.417	32.67±1.74
25%Cops/ABS	2.8±0.4	1.682±0.471	26.13±2.85
2.5%Maps/ABS	15.1±3.4	1.170±0.280	34.14±4.61
5%Maps/ABS	16.7±5.8	1.192±0.292	34.22±2.04

15%Maps/ABS	5.8±2.3	1.722±0.125	36.27±2.51
25%Maps/ABS	3.7±0.5	1.764±0.897	37.52±5.32

Since many of the early published results, especially on polypropylene and polyamide-6, have shown enhanced mechanical properties due to nanocomposite formation, this is apparently now the expectation. In previous work from these laboratories, it has been shown that this is not always the case for both styrene and methacrylate [16]. These data confirm this observation and suggest that more work needs to be done to understand the relationship between nanocomposite formation and mechanical properties.

4. Conclusions

Both of these polymeric clays offer an advantage in thermal stability when compared to conventional ammonium salts. The degradation begins at higher temperatures for these systems and this may enable melt processing of polymers which require higher temperature, especially the styrene copolymer, COPS. It is clear from the TEM results that the styrene copolymer gives nanocomposites in which one can see individual clay layers while the methacrylate copolymer gives some mixture of immiscible and intercalated nanocomposites. It is no surprise to observe that the thermal stability, as measured by TGA, is higher for the COPS systems than for the MAPS systems, since styrene is inherently more thermally stable than is methyl methacrylate. The peak heat release rate reduction is about the same for both the COPS- and the MAPS-polymer compositions, which shows the presence of nanodispersed clay in the polymer matrix and further indicates that the state of this nanodispersion, intercalated or exfoliated or even if the clay is largely present as clay tactoids, is not important as long as there is good nanodispersion. This is also probably the important factor in mechanical properties, since there is little difference between the two clays. Young's modules does ordinarily increase as the amount of clay increases.

Acknowledgments

This work was performed under the sponsorship of the US Department of Commence, National Institute of Standards and Technology, Grant Number 70NANB6D0119. We thank Peggy Miller, University of Texas Health Center in San Antonio, and Ben Knesek, Southern Clay Products, for obtaining the digital transmission electron micrographs.

References

[1] M. Alexandre, P. Dubois. *Mater Sci Eng*., R28 (2000), pp. 1-6

[2] T.J. Pinnavaia, G.W. Beall ***Polymer-clay nanocomposites.*** Wiley, New York (2001)

[3] Gilman JW, Kashiwagi T, Nyden M, Brown JET, Jackson CL, Lomakin S, et al. In: Al-Malaika S, Golovoy A, Wilkie CA. editors. *Chemistry and technology of polymer additives*, Blackwell Scientific, 1999. p. 249–265.

[4] D. Wang, J. Zhu, Q Yao, C.A. Wilkie. *Chem. Mater*., 14 (2002), pp. 3837-3843

[5] Gilman JW, Kashiwagi T, Giannelis EP; Manias E, Lomakin S, et al. In: Le Bras M, Camino G, Bourbigot S, Delobel R. editors. *Fire retardancy of polymeric materials, the use of intumescence*, Royal Society of Chemistry, Cambridge, p. 203–221.

[6] Su S, Jiang DD, Wilkie CA. Accompanying paper.

[7] Kurata M, Tsunashima Y, In: Brandrup J, Immergut EH, Grulke EA. editors. *Polymer handbook*, 1999, p. VII/1-84.

[8] F.L. Beyer, N.C.B. Tan, A. Dasgupta, M.E. Galvin. *Chem. Mater*., 14 (2002), pp. 2983-2988

[9] Balabanovich AI, Schnabel W, Levchik GF, Levchik SV, Wilkie CA, In: Le Bras M, Camino G, Bourbigot S, Delobel R. editors. *Fire retardancy of polymeric materials, the use of intumescence*, Royal Society of Chemistry, Cambridge, p. 236–251.

[10] Su S, Jiang DD, Wilkie CA. Accompanying paper.
[11] J. Zhu, C.A. Wilkie. *Polym. Int.,* 49 (2000), pp. 1158-1163
[12] J. Zhu, A.B. Morgan, F.J. Lamelas, C.A. Wilkie. *Chem. Mater*., 13 (2001), pp. 3774-3780
[13] J. Zhu, F.M. Uhl, A.B. Morgan, C.A. Wilkie. *Chem. Mater*., 13 (2001), pp. 4649-4654
[14] Uhl FM, Qiang Y, Wilkie CA. Accompanying paper.
[15] Zhang J, Wilkie CA. Manuscript in preparation.
[16] D. Wang, J. Zhu, Y. Qiang, C.A. Wilkie. *Chem. Mater*., 14 (2002), pp. 3837-3843